Clinical Science (2021) **135** 865–884
https://doi.org/10.1042/CS20201366

PORTLAND PRESS

Research Article

Down-regulation of STAT3 enhanced chemokine expression and neutrophil recruitment in biliary atresia

Ming Fu[1,2,*], Ledong Tan[1,*], Zefeng Lin[1], Vincent C.H. Lui[3], Paul K.H. Tam[3], Jonathan R. Lamb[4], Yan Zhang[1], Huimin Xia[1], Ruizhong Zhang[1] and Yan Chen[1,3]

[1]Provincial Key Laboratory of Research in Structure Birth Defect Disease and Department of Pediatric Surgery, Guangzhou Women and Children's Medical Center, Guangzhou Medical University, Guangzhou, Guangdong, China; [2]First Affiliated Hospital of Jinan University, Guangzhou, China; [3]Department of Surgery, The University of Hong Kong, Hong Kong SAR, China; [4]Department of Life Sciences, Faculty of Natural Sciences, Imperial College London, London, U.K.

Correspondence: Ruizhong Zhang (zhangruizhong@gwcmc.org) or Yan Chen (ychenc@hku.hk)

Biliary atresia (BA) is an immune-related disorder and signal transducer and activator of transcription 3 (STAT3) is a key signalling molecule in inflammation. The present study was designed to clarify the function of STAT3 in BA. STAT3 expression was examined in patients and a mouse BA model in which STAT3 levels were further altered with a specific inhibitor or activator. Neutrophil accumulation and the levels of the neutrophil chemoattractants (C–X–C motif) ligand 1 (CXCL1) and IL-8 were determined. The effects of STAT3 inhibition on IL-8 expression were examined in human biliary epithelial cell (BEC) cultures. Functional changes in liver STAT3$^+$ neutrophils in the mouse model were analysed with 10× single cell RNA-seq methods. Results showed STAT3 and p-STAT3 expression was reduced in BA liver tissue compared with control samples. Administration of a STAT3 inhibitor increased jaundice and mortality and reduced body weight in BA mice. In contrast, the STAT3 activator ameliorated BA symptoms. Extensive neutrophil accumulation together with CXCL1 up-regulation, both of which were suppressed by an anti-CXCL1 antibody, were observed in the STAT3 inhibitor-treated group. Recombinant IL-8 administration increased disease severity in BA mice, and the STAT3 activator had the reverse effect. Inhibiting STAT3 increased apoptosis of human BECs together with up-regulated IL-8 expression. RNA-seq analysis revealed reduced the numbers of STAT3 expressing neutrophil in BA which was accompanied by marked enhanced interferon-related antiviral activities. In conclusion, STAT3 reduction, enhanced IL-8 and CXCL1 expression and promoted the accumulation of interferon-responsive neutrophils resulting in BEC damage in BA.

Introduction

Biliary atresia (BA) is a fatal liver disease that occurs primarily in neonates. Although surgery provides a solution for bile drainage, patients often develop progressive liver fibrosis and liver failure without liver transplantation [1]. The aetiology of BA is not fully understood, and immune dysregulation and virus infection appear to contribute to the process. Approximately 20% of BA cases are associated with other congenital malformations, and the presence of multiple cases in a family suggests a genetic predisposition in the disease aetiology, including chromosome abnormalities and genetic polymorphisms [2]. Interestingly, some genes have been suggested to be related to the immune response, such as ICAM1, MIF, CD14, ITGB2 and IFN-γ [3–7]. Although the results of studies vary according to population which further illustrates the complexity of BA aetiology.

*These authors contributed equally to this work.

Received: 16 November 2020
Revised: 18 March 2021
Accepted: 25 March 2021

Accepted Manuscript online: 26 March 2021
Version of Record published: 09 April 2021

Clinical Science (2021) **135** 865–884
https://doi.org/10.1042/CS20201366

Biliary epithelial cells (BECs) or cholangiocytes are active immune cells that play an important role in the BA and many other hepatobiliary diseases [8]. The pathology of BA includes the accumulation of inflammatory cells, damage and blockage of bile ducts, and liver fibrosis. Progression is irreversible even with the clearance of pathogens such as viruses or bacteria or after the Kasai procedure. However, the details of the mechanism are still not fully understood. A recent study by Luo et al. [9] using bioinformatics analysis of cholangiocyte-related inflammatory conditions such as BA, primary biliary cholangitis and primary sclerosing cholangitis found 34 core genes related to intestinal and hepatobiliary diseases. Among them, signal transducer and activator of transcription 3 (STAT3) plays a central role in liver fibrosis [9], though no detailed functional studies have yet been performed.

STAT3 is a transcription factor essential for many physiological responses, and deletion of STAT3 is embryonically lethal [10]. STAT3 is also a key regulator in the haematopoietic and immune systems, as it regulates granulopoiesis and the development and functioning of dendritic cells, T cells and B cells [11]. Multiple signalling pathways of STAT3 have been described. For example, IL-6-STAT3 signalling induced by lipopolysaccharide (LPS) is involved in immune regulation [12], and IFN-γ-mediated STAT3 activation by G-CSFR is related to monocyte differentiation during granulopoiesis [13]. Thus, various biological outcomes of STAT3 signalling may contribute to the phenotypes of different diseases. Changes in *STAT3* polymorphisms are associated with a variety of autoimmune diseases, such as multiple sclerosis, autoimmune thyroid disease, Graves' disease and Crohn's disease. Huang et al. showed the reduction of phospho-STAT3 and ultimately diminished the expression of hepcidin in the liver of late stage of BA which was caused by accumulation of hydrophobic bile acid glycochenodeoxycholate [14]. The study highlights the close relationship of BA and STAT3 and supports further studies on the effects of immune regulation on the pathogenesis of BA.

Neutrophils are important myeloid cells. The effects of *STAT3* on neutrophil functions such as maturation, mobilisation and migration have been reported [15,16]. In an acute inflammatory response, granulocyte colony-stimulating factor (G-CSF) activates the JAK/STAT pathway to promote the maturation and chemotaxis of neutrophils. However, in STAT3-deficient mice, a large accumulation of neutrophils can still be found in the lesion area. The accumulation of neutrophils in the animal model of BA was observed [17]. This finding prompted us to investigate the potential role of STAT3 in the pathology of BA in patient samples and in a BA animal model using inhibitors and activators of STAT3. The effects of modulating STAT3 on expression of neutrophil chemoattractant chemokine (C–X–C motif) ligand 1 (CXCL1) in an animal model and on IL-8 biosynthesis in human BEC cultures were also explored. The results suggest that STAT3 contributes to the disease process in BA and provide new information to enhance the understanding of BA pathogenesis.

Materials and methods

Reagents and antibodies

All chemical reagents were purchased from Sigma (Sigma–Aldrich Corp., St. Louis, U.S.A.) unless otherwise stated. The reagents and antibodies used in the experiments were listed in Supplementary Table S1.

Patient subjects

Fresh BA liver tissue (n=28, average age: 2.6 months) was obtained from wedge biopsies collected from patients undergoing intraoperative cholangiograms and the Kasai operation. Control samples were obtained from patients with choledochal cysts (CC) (n=20, average age: 9.1 months) (Supplementary Table S2). All fresh liver tissues were collected from Guangzhou Women and Children's Medical Center, China. The diagnosis of BA was confirmed by histological evaluation of the liver and the portal plate, which demonstrated bile duct obstruction. The human study protocols, which conformed to the ethical guidelines of the 1975 Declaration of Helsinki, were approved by the institutional review boards of Guangzhou Women and Children's Medical Center, China (2017021302) and all subjects had signed written informed consent before the study. All tissue samples for histological study and immunohistochemical staining analysis were obtained from the Department of Pathology and the Biobank of the hospital. For single-nucleotide polymorphism (SNP) analysis, tissue samples were collected during surgical procedures performed on 503 sporadic BA patients recruited between 2000 and 2015. At the time of sample collection patient details including their birthplace and if any close family or relative has the disease were collected as a part of medical history. Blood samples were collected from 495 geographically and ethnically matched controls with no history of BA or related hepatobiliary disorders.

Animal model establishment and treatment

The BA mouse model with rhesus rotavirus (RRV) inoculation was used in the experiments. The RRV strain MMU 18006 was purchased from American Type Culture Collection (ATCC, Manassas, VA, U.S.A.). MA104 cells were used to amplify the virus, which was quantified by a plaque assay as described previously. Pregnant BALB/c mice were purchased from Guangdong Animal Experimental Center and kept in a specific pathogen-free room with a 12-h dark–light cycle. Neonatal BALB/c mice were intraperitoneally injected with 20 μl of 1.5×10^6 pfu/ml RRV within 24 h of birth to establish the experimental BA model or with supernatant from the MA104 cell cultures as a control. Infected mice that died within the first 2 days or not fed by their mothers were excluded from further analysis. The experimental protocol was approved by The Institutional Animal Care and Use Committee of Jinan University Laboratory Animal Center (#IACUC-20180705-12), and the animal experiments were carried out in the Laboratory Animal Management Center of Jinan University. The animals were given anaesthesia with pentobarbital sodium (50 mg/kg) and at the end of the experiments and an overdose of pentobarbital sodium (200 mg/kg) was given before the sample collection.

The mice were randomly separated into control (Cont.) and treatment groups. For the drug treatment group, the STAT3 inhibitor Stattic (25 μg/g, Santa Cruz Biotechnology) and the STAT3 activator Colivelin (1 μg/g, Santa Cruz Biotechnology, Inc., TX, U.S.A.) were given 4 h before RRV inoculation and within 24 h after birth. The vehicle control of DMSO/PBS was given to BA mice and no toxicity effect was observed. The chemotactic cytokine IL-8 (50 ng/mouse, BioLegend, CA, U.S.A.) and an CXCL1 antibody or an IgG2b isotype control (10 μg/mouse, Thermo Fisher Scientific, MA, U.S.A.) were administered at the same time. BA symptoms were monitored and recorded. For tissue sample collection, mice were dissected under a microscope (SMZ1000, Nikon); injection of 0.4% Methylene Blue into the gallbladder was used to test for blockage of the bile ducts, and the liver was photographed. Samples were collected and fixed in 10% formalin for histological study or kept in −80°C for RNA or protein isolation.

Extrahepatic cholangiography

At the end of the experiments, the mice were anaesthetised with Sevoflurane. The liver, gallbladder and extrahepatic bile ducts were fully exposed with a cotton swab, and the appearance of the liver and bile ducts were observed and photographed under a dissection microscope. Then, ophthalmic forceps were used to gently hold the bottom of the gallbladder, slowly inserting a 1-ml syringe needle with Methylene Blue solution (0.05 wt. % in H_2O) into the gallbladder cavity, grasping the needle with ophthalmic forceps, and slowly infusing 10–20 μl of Methylene Blue. Finally, the extrahepatic bile ducts were observed and photographed under a microscope.

Histological analysis and immunohistochemical staining

Liver tissue samples from either human patients or animals were fixed in formalin overnight and embedded in paraffin. Four-micron-thick tissue sections were stained with Haematoxylin and Eosin (HE) for histological analysis. Picrosirius Red staining was used to detect the collagen deposition of liver fibrosis. After Haematoxylin counterstaining, the tissue section was treated with Picrosirius Red for 1 h at room temperature; the sections were then mounted and analysed. For immunohistochemical staining, antigen retrieval was performed in citrate buffer (10 mM, 0.01% Tween 20, pH 6.0) for CK19 or Tris-EDTA buffer (10 mM Tris Base, 1 mM EDTA solution, pH 9.0). Endogenous peroxidase activity was blocked by 3% hydrogen peroxide treatment. The sections were then incubated for 30 min in a blocking solution (antibody diluent, Dako), followed by an overnight incubation at 4°C in the blocking solution containing primary antibodies. The antibodies used were anti-STAT3 (1:50) and anti-p-STAT3 (Tyr^{705}, 1:50) antibodies from Cell Signaling (MA, U.S.A.), an anti-p-STAT antibody (Ser^{727}, 1:50) from Abcam and an anti-CXCL1 antibody (Thermo Fisher Scientific, 1:50). ImmPACT DAB (VECTOR, CA, U.S.A.) was used for development. The results were analysed using a Nikon microscope (Eclipse Ci, NIKON, Japan) and captured with NIS-Elements F4.0 (Nikon). For quantification of the tissue sections, six to ten individual sections were used for each group and five fields around the portal area in each section were photographed blinded and counted with NIH software ImageJ (NIH, Maryland, U.S.A.).

Flow cytometric analysis

Fresh mice livers were collected, and the tissue samples were gently minced though a 70-μm cell strainer. After washing with RPMI 1640 medium (Thermo Fisher Scientific, MA, U.S.A.), lysis buffer (Thermo Fisher Scientific) was added to remove red blood cells. After gradient centrifugation with Percoll (GE, CT, U.S.A.), the single-cell suspension of hepatic mononuclear cells was analysed by cytometry. The antibodies used or flow cytometric analysis were purchased from Thermo Fisher Scientific, including anti-mouse CD11b-FITC, anti-mouse Gr-1-PE/FITC, anti-mouse Ly6G-PE, anti-mouse Ly6C-PerCP-Cyanine5.5, anti-mouse CD4-PerCP-Cyanine5.5, anti-mouse CD3e-Alexa Fluor

Clinical Science (2021) **135** 865–884
https://doi.org/10.1042/CS20201366

488, anti-mouse CD8a-APC, anti-mouse MHC-II-PE, anti-mouse F4/80-APC and anti-mouse CD11c-PE. The results were analysed using FlowJo software (FlowJo LLC, OR, U.S.A.).

Protein quantification with Western blotting

Liver tissue was lysed with RIPA lysis buffer in the presence of 100 mM PMSF (Sigma). After centrifugation, quantification of the protein in the supernatant was performed with a Pierce™ BCA protein assay kit (Thermo Fisher Scientific). Fifty micrograms of protein was added to each well, and the proteins were separated by SDS/PAGE. After the proteins were transferred to a PVDF membrane, the membrane was incubated with a primary antibody overnight, followed by HRP-conjugated secondary antibody staining. Signals were revealed with Immobilon Western Chemiluminescent HRP Substrate (Millipore, MA, U.S.A.). Anti-STAT3 and anti-p-STAT3 antibodies (1:1000, Cell Signaling) were used, and the results were analysed with Bio-Rad ChemiDoc™ Imaging System (Bio-Rad Laboratories, Inc., CA, U.S.A.).

Gene expression analysis with reverse transcription polymerase chain reaction

Total RNA was extracted with RNeasy Mini Kit (Qiagen, Hilden, Germany). One microgram of RNA was used for reverse transcription with the iScript™ gDNA Clear cDNA Synthesis Kit (Bio-Rad). Expression of human *STAT3* was detected using SYBR Green Supermix (Bio-Rad) with Quant Studio™ 6 Flex System (Applied Biosystems, CA, U.S.A.). For the Q-PCR, the polymerase activation and cDNA denaturation were set at 95°C for 30 s. Amplification is through denaturation at 95°C for 15 s and then annealing at 60°C for 60 s with 40 cycles. The following primers were used: human *STAT3*: forward, 5′-AGCAGCACCTTCAGGATGTC-3′, and reverse, 5′-GCATCTTCTGCCTGGTCACT-3′; mouse CXCL1: forward, 5′-ACTGCACCCAAACCGAAGTC-3′, and reverse, 5′-TGGGGACACCTTTTAGCATCTT-3′; human *IL-8*: forward, 5′-TTTTGCCAAGGAGTGCTAAAGA-3′, and reverse, 5′-AACCCTCTGCACCCAGTTTTC-3′; human β-actin: forward, 5′-ACCCACACTGTGCCCATCTAC-3′, and reverse, 5′-TCGGTGAGGATCTTCATGAGGTA-3′; and mouse β-actin: forward, 5′-AAACTGGAACGGTGAAGGTG-3′, and reverse, 5′-AGTGGGGTGGCTTTTAGGAT-3′.

BEC cultures

Human intrahepatic BECs were purchased from ScienCell (ScienCell, CA, U.S.A.). The passage 3–4 was used in the study. The cells were cultured in epithelial cell medium (EpiCM, ScienCell) with 2% (v/v) FBS, 1% (v/v) epithelial cell growth factors (EpiCGS, 4152, ScienCell) and 1% (v/v) penicillin–streptomycin (Thermo Fisher Scientific) in a 5% CO_2 incubator.

Human neutrophil and BEC co-cultures

Human peripheral blood was collected and gradient centrifuged with a Histopaque-1119/Histopaque-1077 mixture. Prior to use in experiments, the layer of neutrophils from the Histopaque gradient was transferred to a new tube, treated with red blood cell lysis buffer, centrifuged and washed with PBS. To test the effects of activating neutrophils with BECs, BECs (3×10^5/well) were seeded and cultured for 48 h. The neutrophils were preactivated with 0.1 μM phorbol 12-myristate 13-acetate (PMA; Sigma–Aldrich) for 20 min. To remove the PMA, cells were centrifuged at 500×*g* for 5 min and the supernatant containing PMA was carefully removed before the neutrophils were cocultured with the BECs. For the control group, the same volume of DMSO was used. Each experiment has been repeated a minimum of three times. The cells were cultured for 24 or 48 h and then photographed.

Liver neutrophil isolation and 10× single-cell RNA-seq analysis

The livers from the NC and BA groups of mice were collected on day 5 and digested into single cell suspensions using the Liver Dissociation Kit (Miltenyi Biotec Inc., CA, U.S.A.) following the instructions of the Gr-1$^+$ Cell Magnetic Bead Separation Kit (Miltenyi). In brief, after FcR blocking single cells were incubated with anti-Gr-1-Biotin. Then after further washing the cells were incubated with anti-Biotin MicroBeads and the Gr-1$^+$ cells were sorted on a MACS® Separator (Miltenyi). The purity of the Gr-1$^+$ cell was over 90% flow cytometry. The viability of the cells used in 10× Genomics single-cell RNA-sequencing was greater than 90%. RNA-seq library preparation for 10× Genomics single-cell 3′ was achieved by mixing Gr-1$^+$ cells with the RT-PCR master mix and gel beads containing barcode information and enzymes, and reverse transcribed to synthesise labelled cDNA according to the manufacturer's instructions. The cDNA was ultrasonically broken into fragments (200-300 bp) and the sequencing adapter P5 (Illumina P5

adapter: 5′- AATGATACGGCGACCACCGAGATCTACAC-3′) and sequencing primer R1 (5′- ACACTCTTTCCC-TACACGACGCTCTTCCGATCT -3′) were added and PCR amplification was performed to obtain a DNA library.

The original data were analysed using 10× single-cell RNA-seq configuration analysis software Cell Ranger (3.1.0) to demultiplex the cellular barcodes and align reads to the mm10 mouse reference genome. For data quality control, cells with fewer than 200 genes or more than 5000 genes detected, and cells for which more than 5% of UMIs were derived from mitochondrial genes or haemoglobin (HB) genes were excluded. Following the quality control procedure, the dataset consisted of 8351 cells expressing 16738 genes. The Seurat package was used to normalise data, dimensionality reduction, clustering, differential expression. Seurat alignment method canonical correlation analysis (CCA) was used for integrated analysis of datasets. For clustering, highly variable genes were selected and the principal components based on those genes used to build a graph, which was segmented with a resolution of 0.6. Based on filtered gene expression matrix by Seurat, differentially expressed genes (DEGs) and specific marker genes for each of the cellular were using Seurat's *FindMarkers* function. Detailed of the cellular subsets and their marker genes are included in the figures and main test of the relevant sections. Loupe Cell Browser 5.0.0 was used to visualise the Cell Ranger data. Further pathway analysis was performed using the Metascape tool [18].

SNP genotyping and quality control

SNP rs7211777 was chosen to identify susceptibility to disease. The MassARRAY iPLEX Gold system (Sequenom) was selected for genotyping of all samples, including 503 cases and 495 controls. PLINK1.9 (genotype test of 3 × 2 contingency tables, Cochran–Armitage trend test, test of dominant and recessive models) was used to compare the difference in allele frequency between patients and controls.

Statistical analysis

All clinical data are presented as the mean ± standard deviation (SD). Statistical analysis was performed using GraphPad Prism software, version 8.0 (GraphPad Software, San Diego, CA). Student's *t* test was applied when comparing two sets of data and one-way analysis of variance (ANOVA) when three or more sets were compared. Tukey's multiple-comparison test was used for statistical analysis of each individual comparison within a group. *P*-values less than 0.05 were considered statistically significant.

Results

Expression of *STAT3* in liver tissues of BA patients

The pathological characteristics of the BA were present namely abnormal bile duct morphology, extensive inflammatory cell infiltration (Figure 1A) and increased tissue fibrosis (Figure 1B). To explore the expression of *STAT3* in BA patients, liver tissue samples from BA (n=28) and CC (n=20) cases were analysed and compared. *STAT3* mRNA expression in CC was distributed widely, but in BA, it was present as a tight cluster and was two-fold lower (P<0.001) (Figure 1C). The protein levels and activation state of STAT3 were examined by Western blotting. In BA, the levels of both total STAT3 and the active form p-STAT3 were lower than the corresponding levels in CC (Figure 1D). Immunohistochemical staining indicated that STAT3 was largely expressed in hepatocytes in CC, whereas in BA much less staining was observed and was present in hepatocytes and portal areas. In addition, p-STAT3 was detected only in inflammatory cells and BECs in CC but was nearly absent from BA (Figure 1E).

Effects of inhibiting or activating STAT3 in the BA mouse model

The effect of altering STAT3 activity was examined using the RRV-inoculated BA mouse model and a STAT3 inhibitor and activator. Morphological analysis showed that inhibition of STAT3 by the specific inhibitor Stattic increased the severity of BA symptoms (Figure 2A,B), with jaundice appearing earlier on day 5 as compared with day 6 or 7 after virus inoculation alone. The mean survival time (MST) was reduced from 15 to 9.5 days (Figure 2C). A further reduction in body weight was observed when Stattic treatment (n=10) with RRV inoculation was compared with RRV inoculation (n=8) alone, but with no statistical significance (Figure 2D). Pathological investigation showed an increase in inflammatory cells in the portal areas in the Stattic treated group (Figure 2E). In contrast, compared with RRV only, the application of the STAT3 activator Colivelin (n=6) ameliorated BA by increasing survival time (from 15 to over 25 days), and body weight also increased slightly (Figure 2C,D). Inflammatory cell infiltration was greatly reduced in the Colivelin group (Figure 2E). Additional representative morphological changes are shown in Supplementary Figure S1.

Clinical Science (2021) **135** 865–884
https://doi.org/10.1042/CS20201366

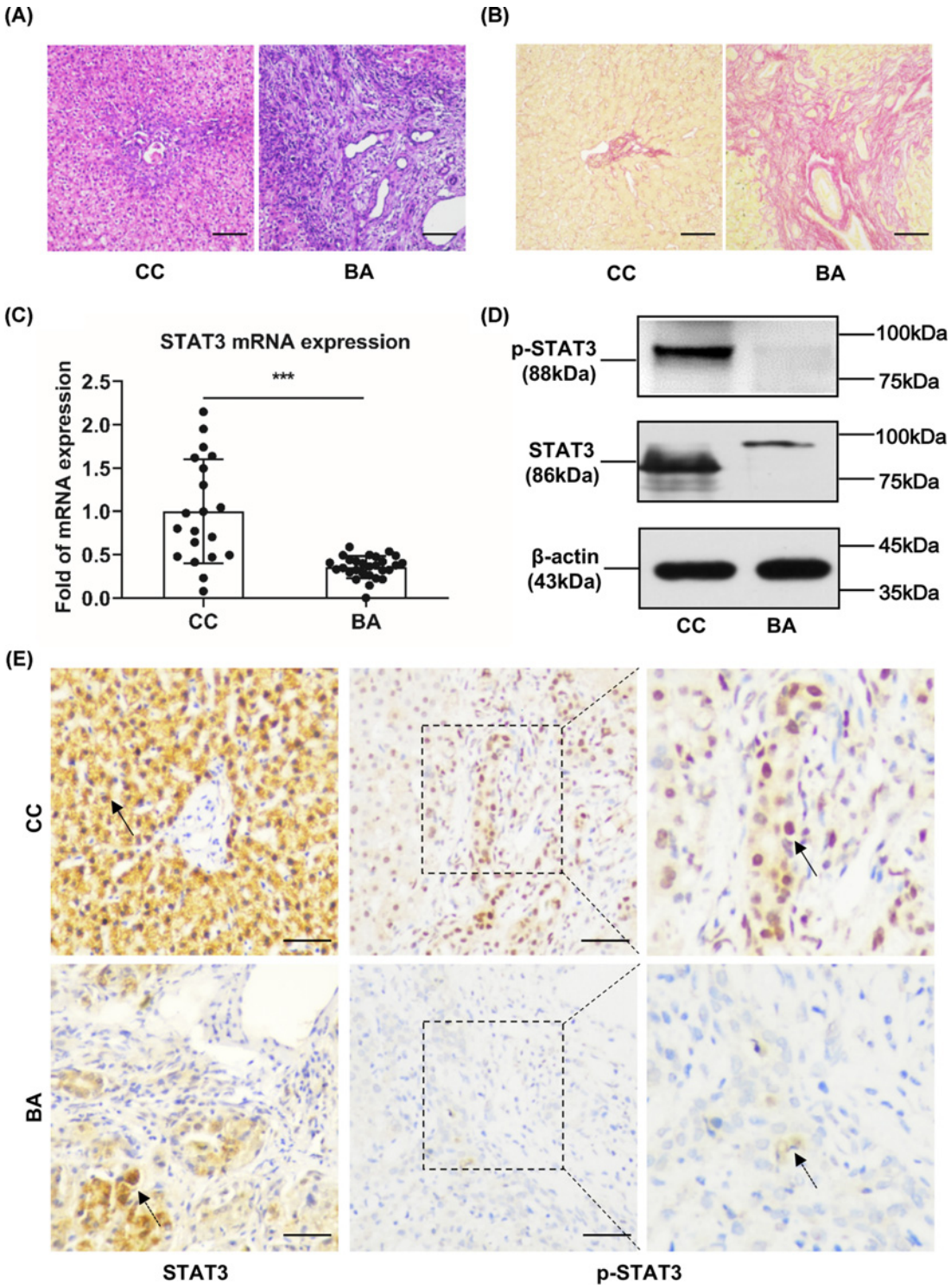

Figure 1. Tissue fibrosis and the expression of STAT3 in BA

(**A**) HE staining showed the cellular infiltrate in CC and BA patient liver samples. The scale bar represents 50 μm. (**B**) Picrosirius Red staining shows fibrosis in CC and BA patient liver samples. (**C**) mRNA expression of *STAT3* measured by quantitative PCR. ***$P<0.001$ ($n=20$ for CC and $n=28$ for BA). (**D**) Protein expression of STAT3 and the activated form p-STAT3 determined by Western blotting. $N=4$ for both CC and BA; one set of representative results is shown. (**E**) Immunohistochemical staining showed expression of STAT3 and p-STAT3 in BA and CC patient liver samples. The portal areas are shown, and the arrows indicate the positions where BECs can be observed. The solid arrows indicate these features in the CC samples, and the dashed arrows indicate these features in BA. The scale bar represents 50 μm.

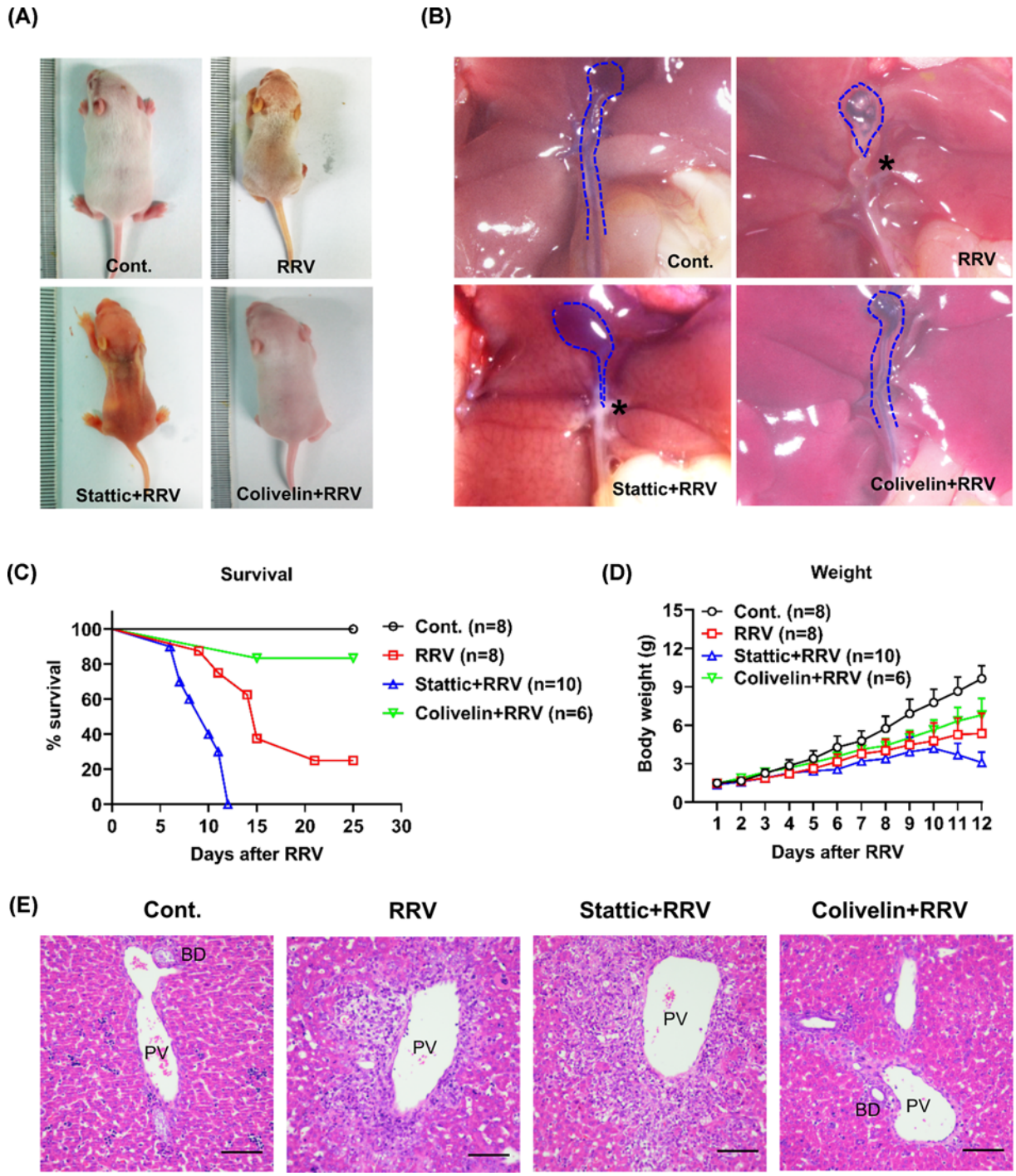

Figure 2. Effect of STAT3 inhibition and activation on a mouse model of BA

The STAT3 inhibitor Stattic (25 μg/g body weight, n=10) or activator Colivelin (1 μg/g body weight, n=6) was given 4 h before RRV inoculation, and mouse morphology, body weight and survival time were recorded. (**A**) Effects of Stattic and Colivelin on BA syndrome. Photographs of the mice were taken on day 9 after RRV inoculation. (**B**) Photographs of the portal areas after dissection under a dissecting microscope. Cholangiography was achieved by injection of 0.4% Methylene Blue. The dashed blue line shows the outline of the gallbladder and bile duct. The asterisks depict BA. (**C**) Effects of Stattic and Colivelin on BA mouse survival. (**D**) Effects of Stattic and Colivelin on BA mouse body weight changes. (**E**) HE staining showing the hepatic bile ducts and cellular infiltration in the Stattic and Colivelin treatment groups. The scale bar represents 50 μm. Abbreviations: BD, bile duct; PV, portal vein.

Clinical Science (2021) **135** 865–884
https://doi.org/10.1042/CS20201366

Inhibition of STAT3 altered the proportion of immune cell types in BA

The immune cells in BA mice treated with the STAT3 inhibitor were analysed using flow cytometry on days 3, 6 and 9 after they were inoculated with RRV. On day 3, there were increases in all immune cells examined, such as natural killer (NK) cells ($P<0.05$) and $CD4^+$ T cells ($P<0.05$). However, following inhibition of STAT3 with Stattic on day 3 after RRV inoculation we observed increased numbers of innate immune cells, including NK cells ($P<0.001$), macrophages ($P<0.01$), neutrophils ($P<0.05$) as well as adaptive immune cells namely $CD4^+$ T cells ($P<0.01$) and $CD8^+$ T cells ($P<0.05$), (Supplementary Figure S2A,D). A significant increase in the number of all inflammatory cell types analysed was also observed on day 6 in the RRV inoculation mice compared with the controls ($P<0.001$). Treatment with Stattic further increased the accumulation of macrophages, neutrophils, $CD4^+$ T cells and $CD8^+$ T cells ($P<0.001$). In contrast, there was a reduction in NK cell accumulation, but no significant differences were observed ($n=3$ in each group; Supplementary Figure S2B,E). Similar to the changes observed on day 6, the elevated levels of inflammatory cells were maintained on day 9, whereby NK cells, neutrophils, $CD4^+$ and $CD8^+$ T cell levels were significantly higher in the RRV group than in the control group ($P<0.001$ for NK cells, $P<0.05$ for $CD4^+$ T cells and neutrophils and $P<0.01$ for $CD8^+$ T cells). Treatment with Stattic also had an effect on neutrophils in that it increased their number ($P<0.001$), though this treatment significantly reduced the NK cell number compared with the RRV group ($P<0.001$) ($n=3$ in each group; Figure 3A and Supplementary Figure S2C).

In view of the high level of neutrophils present in the BA mouse model, especially following Stattic treatment, their presence was further examined by immunohistochemical staining. A progressively increasing number of neutrophils ($P<0.001$) was observed on all days analysed after RRV inoculation, but there was only a slight increase in the neutrophil number after treatment with Stattic compared with RRV alone, and this difference was not statistically significant. However, administration of the STAT3 activator Colivelin resulted in a reduction in the number of neutrophils on days 3, 6, 9, and 12 ($P<0.01$ on day 3 and $P<0.001$ on days 6, 9 and 12, $n=5$ in each group) (Figure 3B). Extensive immune cell infiltration was observed, and mouse death often occurred on day 12 in the Stattic treatment group. Nonetheless, Colivelin treatment largely ameliorated cellular infiltration and protected the bile duct from RRV-induced damage (Supplementary Figure S3A).

In BA patients, blood examination indicated that the absolute number of neutrophils was increased (4.33E+09±2.4E+09, $n=63$) compared with controls, which included healthy controls (Cont, 2.18E+09±8.68+08, $n=40$), congenital heart disease (CHD, 2.28E+09±9.21E+08, $n=35$; $P<0.001$), infant hepatitis syndrome (IHS, 2.62E+09±1.01E+09, $n=40$; $P<0.001$) and CC patients (CC, 2.88E+09±1.18E+09, $n=40$; $P<0.05$) (Supplementary Figure S3B). Similarly, the percentage of neutrophils in BA patients (37.5 ± 15.6%) was higher than that in other groups: Cont. (22.2 ± 5.6%; $P<0.001$) and IHS (24.5 ± 7.2% $P<0.001$); CC (25.9 ± 7.5%; $P<0.01$) and CHD (26.3 ± 7.6%; $P<0.05$) (Supplementary Figure S3C). In the portal area of liver tissue sections, immunohistochemical staining showed that the number of neutrophils in BA (116.0 ± 8) was higher than that in cavernous transformation of the portal vein (CTPV, 1.4 ± 0.9; $P<0.001$) ($n=5$ in each group; Figure 3C).

Modulation of CXCL1 expression in the BA model after treatment with Stattic and Colivelin

As mice do not have an IL-8 gene, the functional homologue CXCL1 was used to detect changes in the functional effects of neutrophil chemoattractants in response to STAT3 inhibition and activation. Expression of CXCL1 mRNA was examined by Q-PCR in mouse liver tissue. The results revealed that CXCL1 mRNA expression was significantly increased on day 12 ($P<0.001$). Following inhibition of STAT3, elevated CXCL1 expression was observed earlier on day 6 ($P<0.01$), which was maintained on day 9 ($P<0.001$). However, activation of STAT3 by Colivelin did not significantly reduce CXCL1 expression on day 6 or 9 ($P>0.05$) but did on day 12 ($n=3$ in each group; $P<0.001$) (Figure 4A). Next, cells expressing CXCL1 were detected by immunohistochemical staining (Figure 4B). $CXCL1^+$ cells were present in the portal areas and were a component of the cellular infiltrate. On day 3, only the RRV group showed an increase in the number of $CXCL1^+$ cells ($P<0.001$ compared with Cont.), and compared with RRV alone, treatment with either Stattic or Colivelin lowered the number of $CXCL1^+$ cells ($P<0.001$). On day 6, more CXCL1-positive cells were found in the RRV group ($P<0.001$ compared with Cont.), and Stattic further enhanced accumulation of $CXCL1^+$ cells ($P<0.001$). Colivelin treatment reduced CXCL1 expression by more than 50% ($P<0.001$ compared with the RRV group). Similar outcomes were observed on days 9 and 12, but at the later time point, treatment with Stattic caused death ($n=5$ in each group; Figure 4C). The results indicated that reduced expression of STAT3 promotes CXCL1 expression in the portal area.

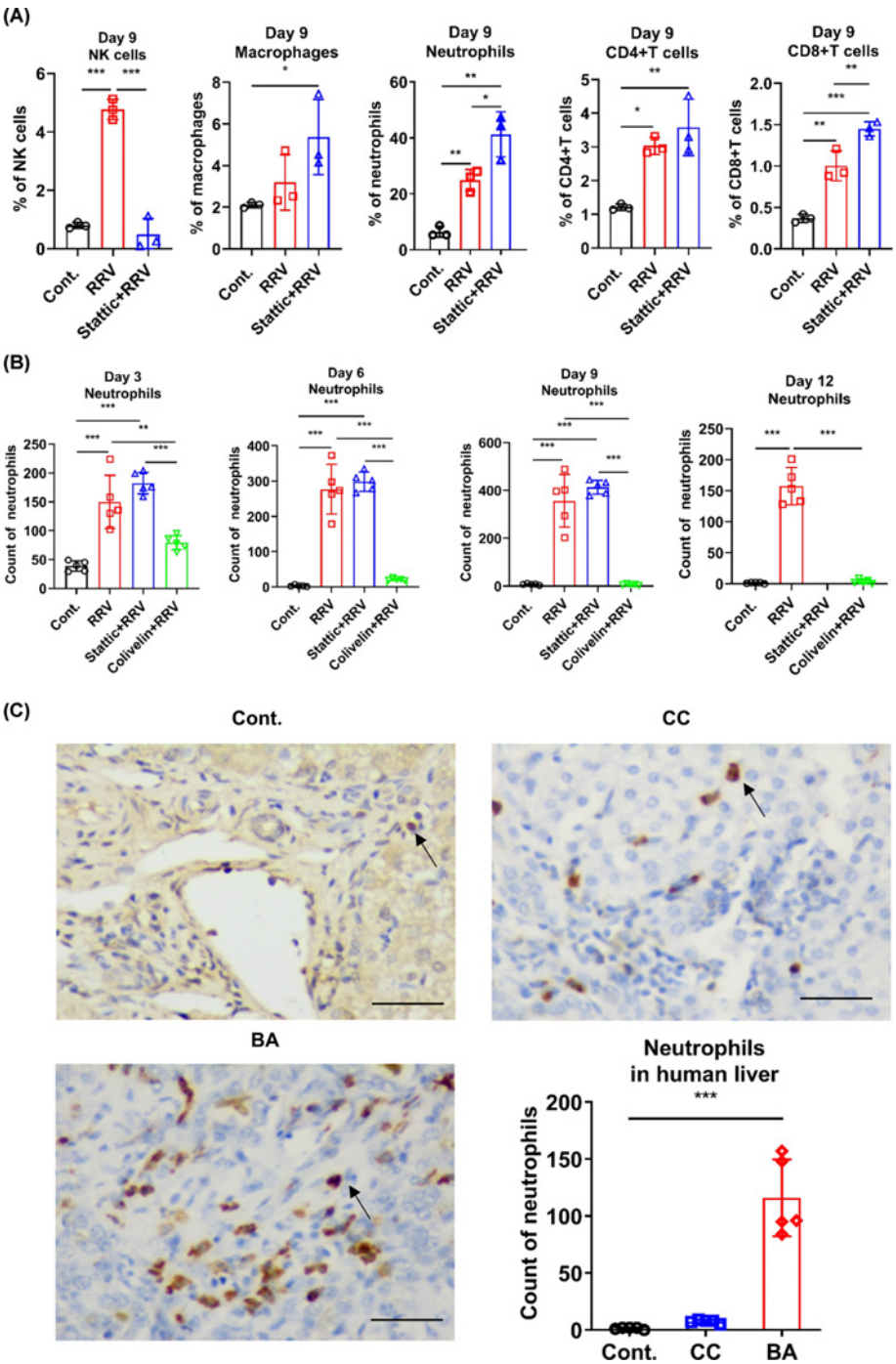

Figure 3. Effects of changes in STAT3 expression on immune cell regulation

(**A**) Effects of STAT3 inhibition on NK cell, macrophage, neutrophil, $CD4^+$ T cell and $CD8^+$ T cell numbers in the liver determined using flow cytometric analysis. Cell suspensions were obtained from the liver at the end of experiments and labelled with the appropriate antibodies for immune cell analysis. At least three sets of experiments were performed, and a representative experiment is shown here. Data were obtained on day 9 after RRV inoculation (other time point analyses are presented in the Supplementary Data). Data were collected from the experiments and evaluated by statistical analysis. $^*P<0.05$, $^{**}P<0.01$, $^{***}P<0.001$. (**B**) Effects of STAT3 inhibition or activation on neutrophil accumulation determined by immunohistochemical staining on days 3, 6, 9 and 12 after RRV inoculation. The number of immune-positive signals was counted, calculated and analysed. $^{**}P<0.01$, $^{***}P<0.001$. (**C**) Immunohistochemical staining of neutrophils in samples from normal controls (transplantation donor liver samples), CC patients and BA patients. The cell numbers in the different categories were evaluated ($n=5$ in the control group, CC and BA groups; $^{***}P<0.001$). The scale bar represents 50 μm.

Clinical Science (2021) **135** 865–884
https://doi.org/10.1042/CS20201366

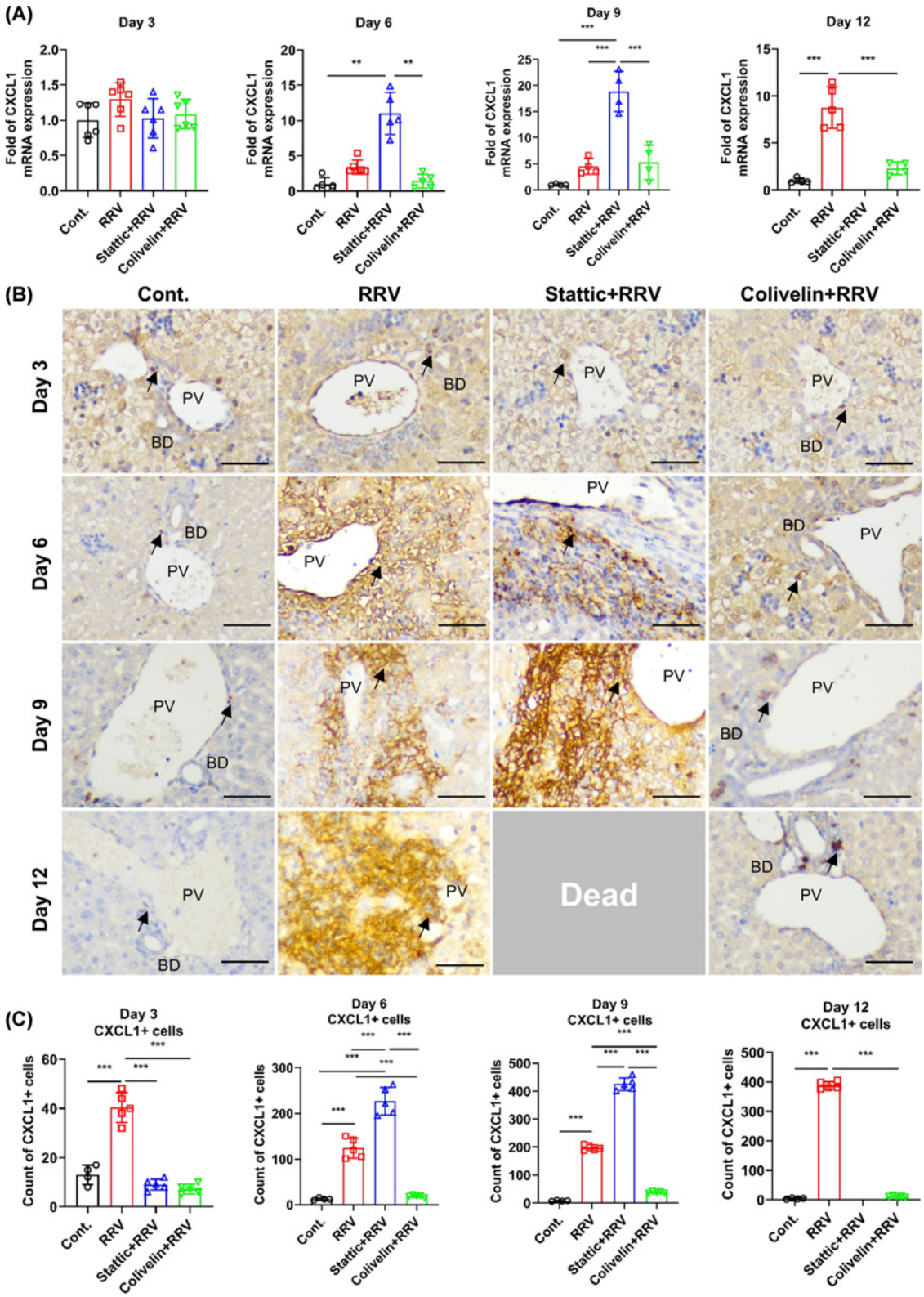

Figure 4. Effect of changes in STAT3 levels on expression of the chemoattractant CXCL1 in a BA mouse model

(**A**) CXCL1 gene expression in response to Stattic or Colivelin treatment was examined by quantitative PCR on days 3, 6, 9 and 12 after RRV inoculation. $^{**}P<0.01$, $^{***}P<0.001$. (**B**) Immunohistochemical staining for CXCL1 was used to assess BA-model mice treated with Stattic and Colivelin. The black arrows represent CXCL1^{+} cells; the scale bar represents 50 μm. (**C**) Immunohistochemical staining and positive cells were quantified and analysed. $^{***}P<0.001$. Abbreviations: BD, bile duct; PV, portal vein.

Effects of a CXCL1 antibody or IL-8 on BA mice with activated or inhibited STAT3

As accumulation of the neutrophils through CXCL1 expression might contribute to disease progression in the BA mouse, we investigated this by targeting CXCL1. The results showed the amelioration of the BA syndrome following anti-CXCL1 antibody (n=10) treatment, as illustrated by an increase in survival times (56% of mice survived for more than 25 days; Figure 5A). Body weight also increased slightly, but this change was not significantly different from the body weight in the RRV group (n=10) on day 12 (Figure 5B). In tissue sections, reduced neutrophil numbers were found at all time points examined (P<0.01 for day 3 and P<0.001 for days 6 and 9 compared with the RRV group; n=5 in each group; Figure 5E). In contrast, the addition of recombinant IL-8, a potent chemoattractant of neutrophils that is absent from mice [19], reduced survival times (the MST was reduced from 15 days in the RRV group to 11 days in the IL-8+RRV group (n=8; Figure 5A), but body weight changes were not significantly different from the results in the RRV group on day 12 (Figure 5B). In addition, the number of neutrophils was only slightly increased in the IL-8+RRV group compared with the RRV group on days 3, 6, 9 and 12 (P>0.05) (n=5 in each group; Figure 5E). Representative images are shown in Supplementary Figure S4.

The STAT3 inhibitor aggravated symptoms of BA in the mouse model. To establish whether this increase in disease severity was due to CXCL1 expression, mice received combined treatment with Stattic (n=10) and the anti-CXCL1 antibody (n=11). The results showed ameliorative effects in terms of survival time (the MST increased from 11 days to 63% of the mice surviving for over 25 days), though there was no obvious improvement in body weight on day 12 (Figure 5C,D). Neutrophil numbers were reduced on days 3, 6 and 9 after treatment (P<0.01 at these time points), but on day 12, the mice receiving Stattic had died (Figure 5E). In contrast, combining Colivelin (n=9) and IL-8 (n=8) reduced symptoms of BA, and both survival time and body weight increased (Figure 5C,D). Furthermore, neutrophil numbers were reduced on days 3, 6 and 9 (P<0.001 for the combined treatment group compared with the IL-8 group; n=5 in each group; Figure 5F). Relative representative images are shown in Supplementary Figure S5.

Activation of neutrophils increases BEC apoptosis

Down-regulation of STAT3 increased neutrophil accumulation in the periductal area. To further investigate whether neutrophils have any effects on BECs, isolated human neutrophils were activated with PMA and co-cultured with BECs. The apoptosis of BEC increased after 48 h of incubation with neutrophils and PMA when compared with neutrophils alone (58.9 $\pm$ 7.4 vs. 3.9 $\pm$ 1.84% and 3.0 $\pm$ 0.6%, both P<0.001 compared with cultures with no neutrophils or non-activated neutrophils; Figure 6A–C). This finding suggests that activated neutrophils have the potential to cause BEC death.

Effects of the STAT3 inhibitor on BEC chemokine expression

The expression of chemokines is a key factor in neutrophil accumulation. Low expression of STAT3 and increased neutrophil numbers in the portal area provide insight into the role of chemokine expression when STAT3 is down-regulated. Examination of IL-8 expression was performed on BEC cultures in the presence of the STAT3 inhibitor Stattic. The results showed cell death after 24 h in the cultures treated with 10 μM Stattic (Figure 7A). To confirm effectiveness of Stattic cells in the other groups were collected 12 h after Stattic was added, and the phosphorylation of STAT3 was measured by Western blotting. The results indicated a reduction in the level of activated STAT3 (p-STAT3) in the presence of 5 μM Stattic, but the effect was less obvious at a concentration of 2.5 μM. Furthermore, treatment with the inhibitor did not change the level of total STAT3 at the time points investigated (Figure 7B,C). IL-8 was detected in BECs treated with 5.0 μM Stattic, and a two-fold increase in IL-8 gene expression was found (P<0.001) (Figure 7D). This increase in the IL-8 level in the supernatant was confirmed by ELISA (P<0.001, Figure 7E). These data suggest that STAT3 might be needed for epithelial cell growth and that disruption of the signalling pathway may induce expression of inflammatory mediators, such as chemoattractants.

Altered gene expression in STAT3$^+$ neutrophils in BA

The expression of STAT3 was analysed in Gr-1$^+$ neutrophils on day 5 after virus inoculation. The percentage of the STAT3$^+$ cells was reduced from 9.1% in the NC group to the 6.8% in the RRV group (Figure 8A). The cells can be further separated to Ly6G$^+$ and Ly6C$^+$ subclusters which reflect G-MDSC and M-MDSC cells present in the neonatal period and they become neutrophil and monocyte respectively after maturation [20]. The percentages of Ly6G$^+$ was three-fold higher than Ly6C$^+$ cells and there were only slight changes in the number of these cells for each cluster in the RRV group (Figure 8B). The percentages of STAT3 were reduced in both Ly6G$^+$ (7.5 to 5.2%) and Ly6C$^+$ (15.0 top 10.4%) clusters (Figure 8C). The number of the cells was counted and shown (Supplementary Table S3).

Clinical Science (2021) **135** 865–884
https://doi.org/10.1042/CS20201366

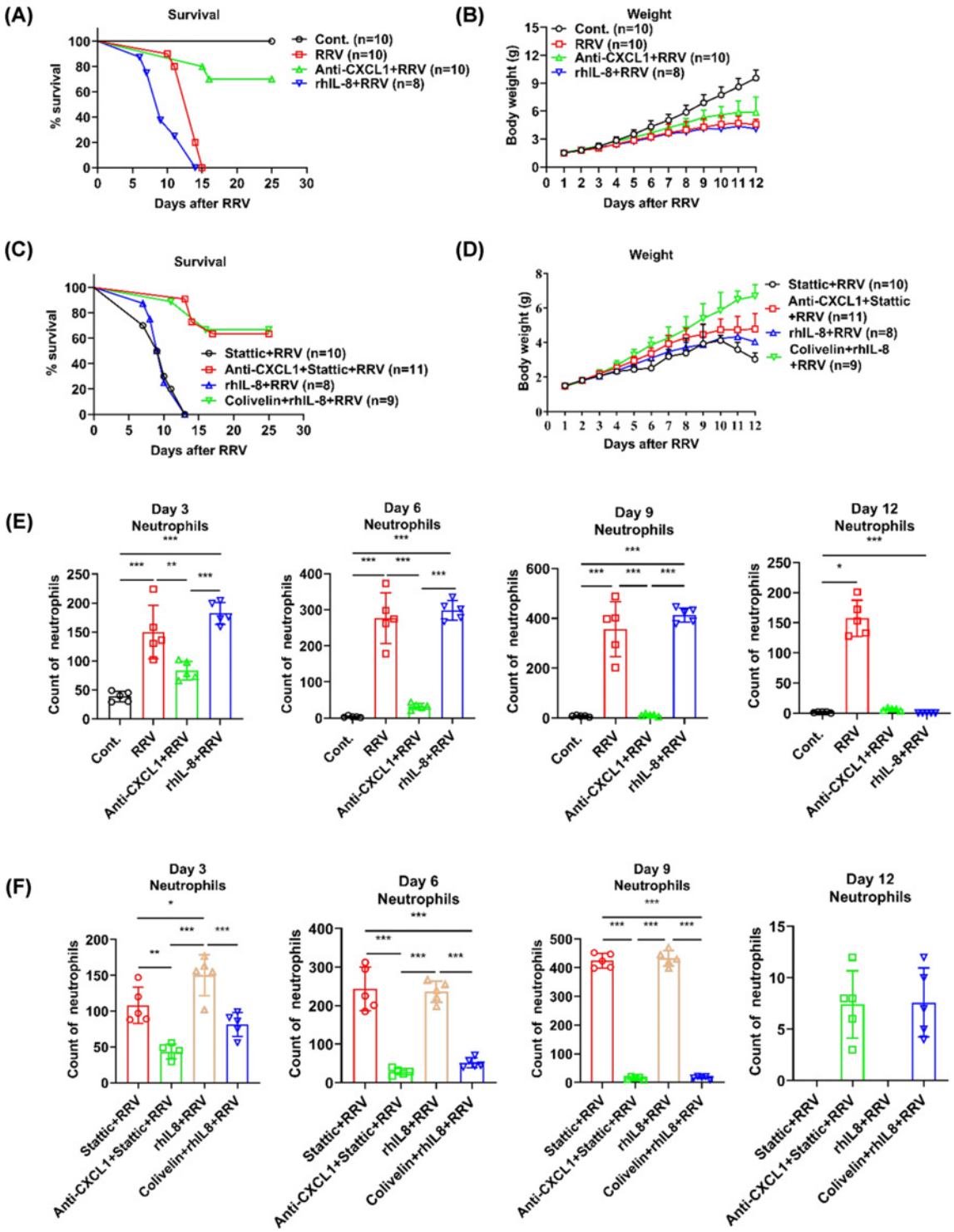

Figure 5. Administration of an anti-CXCL1 antibody or human recombinant IL-8 (rhIL-8) to BA-model mice and the effects of combining the antibody treatment with STAT3 inhibition or activation

(**A**) Changes in survival in BA-model mice induced by an anti-CXCL1 antibody (n=10) or rhIL-8 (n=8) compared with RRV inoculation alone or no treatment. (**B**) The body weight changes corresponding to (A). (**C**) Changes in mouse survival induced by the anti-CXCL1 antibody in the Stattic + RRV group (n=11) compared with the Stattic + RRV group (n=10) and by Colivelin in the rhIL-8 + RRV group (n=9) compared with the rhIL-8 + RRV group (n=8). (**D**) The body weight changes corresponding to (B). (**E**) Neutrophil counts corresponding to (A) determined by immunohistochemical staining with an anti-neutrophil antibody. $^{*}P<0.05$, $^{**}P<0.01$, $^{***}P<0.001$. (**F**) Neutrophil counts for the data in (C) determined by immunohistochemical staining. $^{*}P<0.05$, $^{**}P<0.01$, $^{***}P<0.001$.

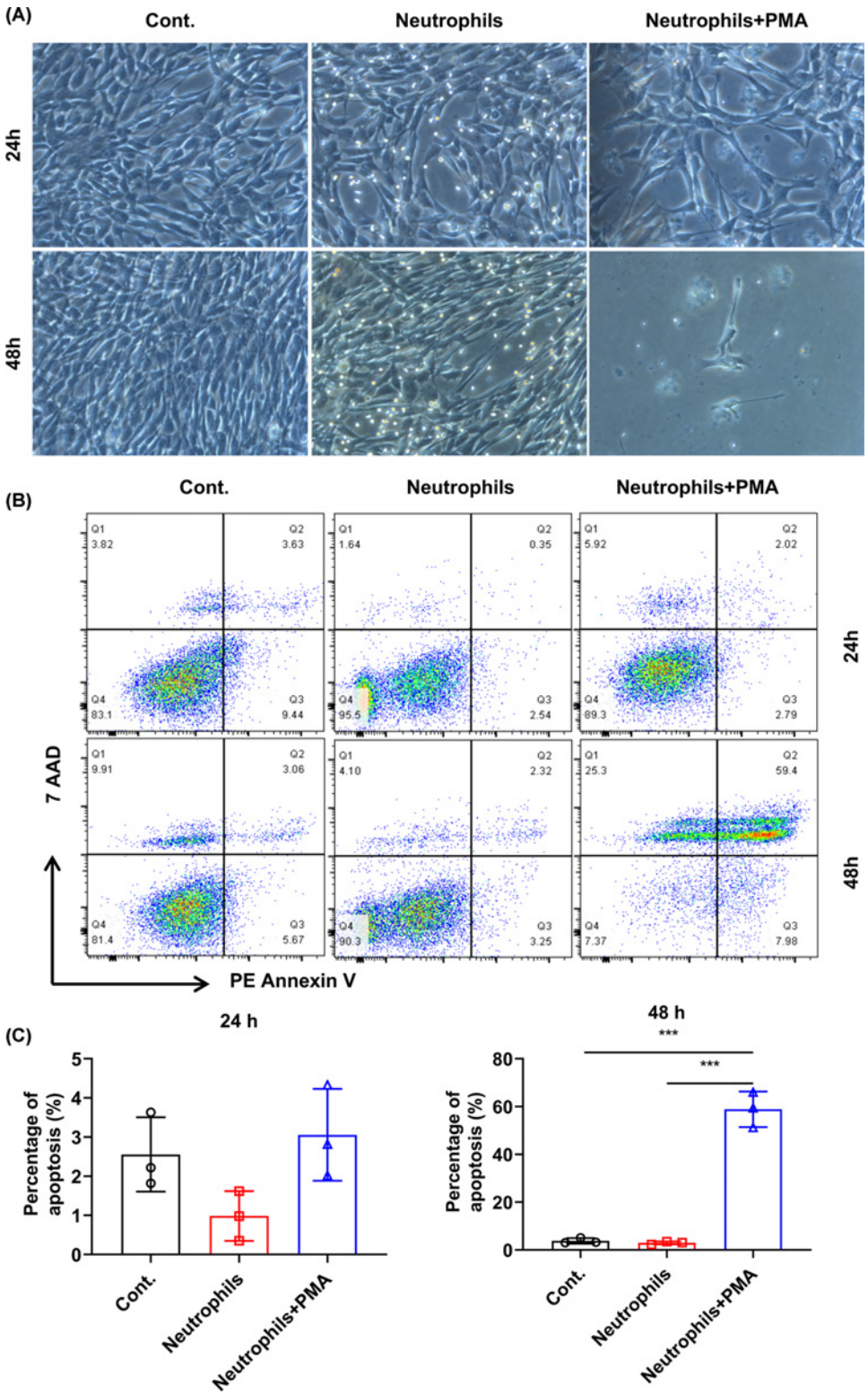

Figure 6. Effects of neutrophil activation on BEC cultures

(**A**) Human BECs were cultured as described previously. Neutrophils isolated from PBMCs were activated with PMA and added to the BEC cultures for another 24 or 48 h, and then the cultures were photographed. (**B**) Apoptosis in single-BEC suspensions cocultured with activated neutrophils was analysed by flow cytometry. At least three sets of experiments were performed, and one representative graph is shown. (**C**) Apoptosis in BECs co-cultured at 24 and 48 h with activated neutrophils was evaluated. ***$P<0.001$.

Clinical Science (2021) **135** 865–884
https://doi.org/10.1042/CS20201366

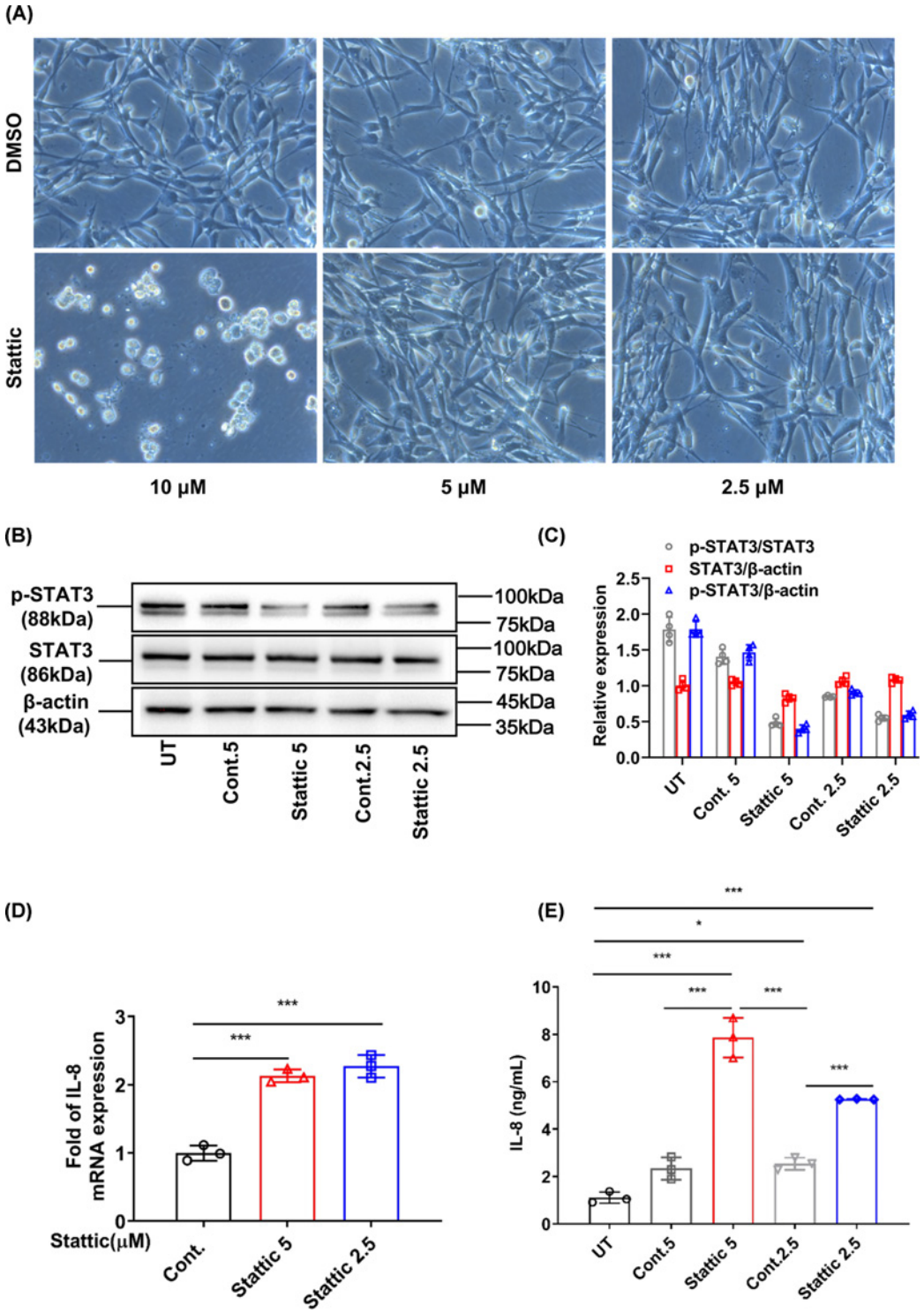

Figure 7. Inhibition of STAT3 in BEC cultures

(**A**) Human BECs were cultured in epithelial cell medium for 48 h, and then different concentrations of Stattic were added to the cultures and incubated for another 24 h before cell morphology was analysed. (**B**,**C**) Western blotting shows the expression of p-STAT3 and STAT3 in cell cultures treated with different concentrations of Stattic for 12 h. Cont., control group with Stattic; Stattic 5, Stattic at a dose of 5 μM. (**D**) mRNA expression of chemoattractant IL-8 in human BEC cultures was measured by quantitative PCR. The cont.2.5 and cont.5 group correspond to the control groups for the STAT3 inhibitor Stattic with 2.5 and 5 μM, with the same volume of DMSO as solvent of Stattic. ***$P<0.001$. (**E**) IL-8 secretion into the supernatant of the cell culture was assessed by ELISA, *$P<0.05$, ***$P<0.001$.

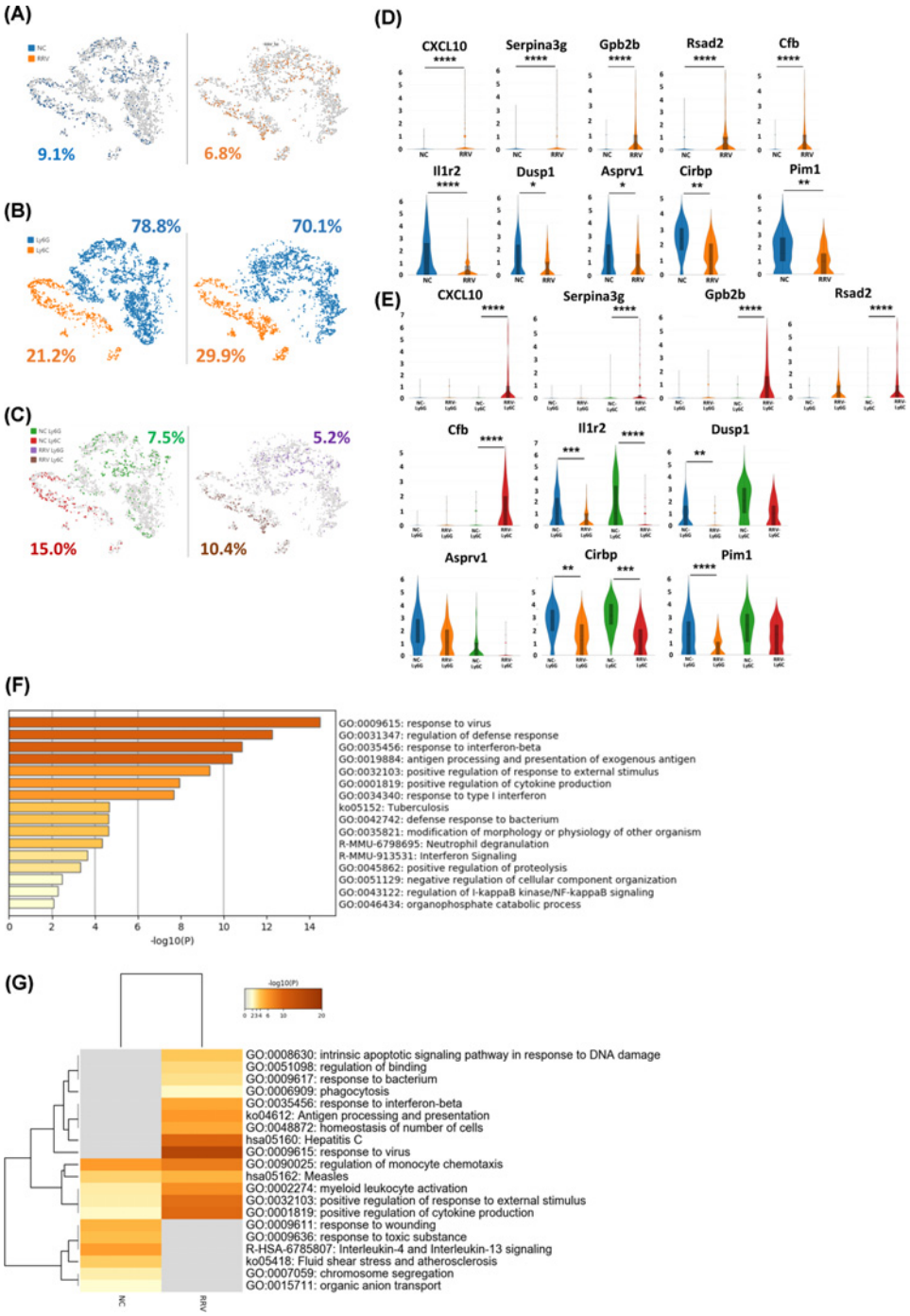

Figure 8. Altered gene expression in STAT3$^+$ neutrophils in BA liver

The 10× single-cell RNA-seq was used in the experiments. (**A**) The results were analysed using Loupe Cell Browser with t-SNE method. The percentages of STAT3$^+$ cells in NC and RRV groups is presented. (**B**) The two subclusters of Gr-1$^+$ cells was showed using Ly6G and Ly6C as markers and the percentage was indicated. (**C**) The expression of STAT3 in each subclusters and the percentage was indicated. (**D**) Five up- and down-regulated genes each in BA compared with the control group. *$P<0.1$, **$P<0.05$, ***$P<0.01$ and ****$P<0.001$, the P-values adjusted using the Benjamini–Hochberg correction for multiple testes was showed in the graph. (**E**) Five up- and down-regulated genes expressed in the sub clusters compared BA and control group with Ly6G$^+$ and Ly6C$^+$indicted. The significant P-value label was the same as previous. (**F**) Metascape analysis showing the enrichment of gene expression in different signalling pathway and interaction of molecules in the context of genes that are highly differentially expressed between NC and RRV groups. (**G**) The analysis of the most highly expressed genes and comparison of the each subcluster to determine functional differences.

Clinical Science (2021) **135** 865–884
https://doi.org/10.1042/CS20201366

However, genes related to the interferon signalling pathway such as *Cxcl10*, *Rsad2*, *Serpina3g* were greatly increased, and in contrast, negative immune regulators such as *Il1r2*, *Cirbp* and were reduced suggesting that the cells were highly activated (Figure 8D). Further analysis found that the up-regulated genes were mostly present in the Ly6C$^+$ population in RRV group but the down-regulated genes were found both in Ly6G$^+$ cells and Ly6C$^+$ cells indicating the differential regulation was due to the virus infection (Figure 8E). These functional changes were confirmed by Metascape analysis and those genes that were markedly different between the NC and RRV groups were related to viral defence responses and the interferon signalling pathway (Figure 8F). In each subcluster similarities in the regulation of defence response and neutrophil degranulation genes were observed. Genes associated with regulation of cells cycle, mitotic cytokinesis were only found in Ly6G$^+$ cells. Whereas those genes regulating leukocyte differentiation and responsiveness to interleukin-1 were present only in Ly6C$^+$ cells indicating functional differences in the response to the virus (Figure 8G). All of these functional activities suggested that neutrophils are active in response to the virus but may also contribute to the damage of the BECs.

Genetic association of *STAT3* with BA

The genetic susceptibility for BA with regard to *STAT3* was examined in southern Chinese populations. SNP rs7211777 was selected for further replication according to the potential regulatory role with *STAT3* expression. As shown in Supplementary Table S4, major allele A of SNP rs7211777 was significantly associated with increased BA risk (OR = 1.61, 95% CI = 1.15–2.25, P=5.31E-03), with a 1.6-fold increased risk. We further explored *STAT3* expression in 36 liver samples with known genotypes and our findings indicated that individuals carrying the disease risk allele A had a significantly lower expression (Supplementary Figure S8A,B; P=0.0071 defined by genotype; P=8.00E-04 defined by allele), which may account, in part, for possible genetic susceptibility to BA.

Discussion

Increased numbers of neutrophils have been observed in BA patients and experimental animal models of BA. In the current study, the down-regulation of p-STAT3 in BA patients and modulation of STAT3 expression with a specific inhibitor or activator in a mouse model of BA resulted in changes in the level of the neutrophil chemoattractant CXCL1. As a consequence, this altered the number of neutrophils present, the symptoms and the pathology. Furthermore, after administration of the anti-CXCL1 antibody, even in the presence of STAT3 inhibitor amelioration of BA was observed suggesting that the main effect of reducing STAT3 was through the augmentation of CXCL1. The use of a STAT3 activator in the presence of recombinant IL-8 also had the beneficial effect of protecting the bile ducts, partly through the inhibition of endogenous CXCL1 expression. However, other functions of STAT3 such as promoting the proliferation of BEC [21] might also contribute to the protective effect on the bile ducts. Collectively, these findings indicate a central role for the STAT3 signalling pathway in the BA disease process.

Hydrophobic bile acids compromise IL-6 signalling through both caspase-mediated down-regulation of gp130 expression and p38 MAPK-dependent inhibition of *STAT3* phosphorylation [22]. Accumulation of bile acid is a feature of BA, however, only a few studies have reported increased IL-6 expression in BA, and from our unpublished data, there were no obvious differences in levels when BA was compared with CC and unrelated disease controls. We observed a reduction in gp130 expression in BA compared with CC by immunohistochemical analysis (data not shown), and less bile acid accumulation was found in CC [23]. Furthermore, in the BA animal model, p-STAT3$^+$ cells were observed on day 9, by which time damage to the bile ducts had already occurred; nevertheless, the p-STAT3$^+$ cells had disappeared by day 12 (Supplementary Figure S6), which suggests that accumulation of bile acid may also reduce STAT3 activity. The effects of STAT3 inhibitor and activation in p-STAT3 was observed in liver section by immunohistochemistry (Supplementary Figure S7).

NK cells play an important role in the BA pathogenesis [24]. However, in this study, the treatment with Stattic significantly reduced the number of NK cells, which was accompanied by increased tissue damage. It has been reported that STAT3 regulates many aspects of NK cell biology, such as NK development, activation and target cell killing [25], and our previous study using silver nanoparticles to inhibit NK cell activity also showed beneficial effects in the BA model [26]. Regardless, the reduction in the NK cell numbers did not result in amelioration of BA in the Stattic-treated group, which might indicate that the increase in neutrophils had a strong promoting effect on the disease. Recent *in vivo* studies have shown that targeted specific knockdown of STAT3 expression in NK cells results in increased NK cell activity through up-regulated expression of DNAM-1 and the lytic enzymes perforin and granzyme B in NK cells, with a beneficial effect against tumour cells [27]. This result indicated the effects that STAT3 might have on different cellular functions depending on the disease model, and further investigation NK cell activity in the BA mouse model treated with Stattic may prove informative.

Previous studies on BA have revealed that a number of molecules may affect the disease process. For example, the pathogen-associated molecular pattern (PAMP) molecule HMGB1 has been shown to have a potent effect on BA by promoting NK cell activation [28]. Zhao et al. also reported up-regulation of HMGB1 expression by rituximab in human diffuse large B-cell lymphoma and suggested that this effect was mediated through the inhibition of STAT3 [29]. Moreover, expression of the long noncoding RNA H19 is up-regulated in both BA patients and an animal model of BA, promoting cholangiocyte proliferation and cholestatic liver injury by regulating the S1PR2/SphK2 and let-7/HMGA2 axis [30]. The effect of H19 has also been investigated in endothelial cell ageing within the context of intercellular adhesion molecule 1 (ICAM1) and vascular cell adhesion molecule 1 (VCAM1) expression, and it was observed that depletion of H19 increased ICAM1 and VCAM1 expression. Overexpression of H19 inhibited STAT3 signalling, whereas depletion of H19 enhanced phosphorylation of STAT3 [31]. Recent studies on the inflammasome in BA have revealed an additional mechanism that contributes to tissue damage, whereby targeted knockdown of expression of NLRP3 and IL-1R1 but not that of caspase 1 protects against bile duct injury [32]. Another study of NLRP3 protein deficiency found enhanced hyperoxia-induced death mediated via STAT3 protein signalling and independent of IL-1β [33]. Furthermore, STAT3 expression is reduced in human neuroblastoma SH-SY5Y cells, which enhances oxidative stress mediated by the NLRP3 inflammasome [34]. Together, these reports suggest that the effects of NLRP3 and IL-1R1 on BA might be related to STAT3 expression.

LPS-enhanced IL-6/STAT3 expression can promote BEC proliferation through activation of p44/p42 MAPK [35], and PD098059, an inhibitor of p44/p42 MAPK, completely blocks proliferation. Regardless, whether STAT3 inhibition has an effect on proliferation has not been explored. Our data indicate that BECs express STAT3 under normal growth conditions and that inhibiting signalling blocks proliferation and induces cell death, indicating that activation of STAT3 is essential for cell growth. Additionally, BECs can produce IL-8 [36], and we report here that it is increased in BEC culture supernatants in the presence of a STAT3 phosphorylation inhibitor. The effect might occur by directly reducing STAT3 repressed IL-8 production or indirectly by enhancing NF-κB promotion of IL-8 expression [37,38]. This result also correlates with high expression of IL-8 detected in BA patients, and has been demonstrated in several clinical studies [39]and in our laboratory (unpublished observations). In conclusion, the findings of the study suggest that STAT3 expression and activation are central in BA pathogenesis.

Gr-1 cells are an abundant inflammatory cell type present in the BA mouse liver and the RNA-seq analysis showed that only 10% of the cells are $STAT3^{+}$ cells in NC group and this was further reduced in BA group. Although there was only a slight reduction in STAT3 expression between the RRV and NC groups their functional activity was markedly different in that IFN-related antiviral effector molecules were greatly increased in the former group. This result suggests that STAT3 may not play a major role in these functional changes. It has been shown the STAT3 deficiency in myeloid cells reduces of bacterial load, but increases neutrophil accumulation [40]. Our data imply that reduced STAT3 expression might not affect the activity of neutrophils, but through the increased chemoattractant production by the BECs, promote the accumulation of activated neutrophils and cause bile duct damage.

A recent study using bioinformatics analysis of human cholangiopathies, including BA, reported modulation by STAT3 expression [9]. Choosing an established eQTL SNP through the GTEX database and identified it as being associated with BA. Interestingly, a significant correlation between the *STAT3* expression level and patients carrying the disease risk genotype (AA) versus patients carrying either of the other two genotypes was observed. However, large sample size is the limitation of the study for the genetic relationship of *STAT3* in BA, which need to further confirm the results especially the potential regulatory susceptibility SNP modulates gene expression is in a tissue-specific manner [11].

Clinical perspectives

- BA is an immune-related disorder with inflammation and tissue fibrosis, but the underlying mechanisms are not clear. STAT3 is a key signalling molecule in inflammation and fibrosis.
- STAT3 expression is reduced in BA patients. In the BA mouse model, the STAT3 inhibitor increased disease severity and the activator reversed BA symptoms. This outcome is, in part, through the regulation of the chemoattractant CXCL1, and the subsequent accumulation of neutrophils which express interferon stimulation. The STAT3 inhibitor induced BEC apoptosis and enhanced expression of IL-8 in cell cultures.

Clinical Science (2021) **135** 865–884
https://doi.org/10.1042/CS20201366

- Our data suggest that in BA a reduction in STAT3 together with enhanced IL-8 and CXCL1 expression promote the accumulation of neutrophils resulting in BEC damage. Potentially the administration of a STAT3 activator might have a beneficial effect in the clinical management of BA.

Data Availability

The authors confirm that the data supporting the findings of the present study are available within the article [and/or] its supplementary materials.

Competing Interests

The authors declare that there are no competing interests associated with the manuscript.

Funding

This work was supported by the National Natural Science Foundation of China [grant numbers 81770510, 81671498, 81974056, 81771629]; and the Science and Technology Planning Project of Guangdong Province [grant number 2019B020227001].

CRediT Author Contribution

Ming Fu: Data curation, Investigation, Methodology. **Ledong Tan:** Data curation, Validation, Investigation. **Zefeng Lin:** Data curation, Formal analysis, Validation, Investigation. **Vincent C.H. Lui:** Conceptualisation, Resources, Writing—review and editing. **Paul K.H. Tam:** Conceptualisation, Supervision. **Jonathan R. Lamb:** Conceptualisation, Supervision, Writing—original draft, Writing—review and editing. **Yan Zhang:** Validation, Investigation, Methodology. **Huimin Xia:** Conceptualisation, Supervision, Funding acquisition. **Ruizhong Zhang:** Conceptualisation, Funding acquisition, Writing—original draft, Writing—review and editing. **Yan Chen:** Formal analysis, Supervision, Funding acquisition, Writing—original draft, Writing—review and editing.

Acknowledgements

The authors would like to thank the Clinical Biological Resource Bank of Guangzhou Women and Children's Medical Center for providing the clinical samples.

Abbreviations

BA, biliary atresia; BEC, biliary epithelial cell; CC, choledochal cyst; CHD, congenital heart disease; CXCL1, (C–X–C motif) ligand 1; G-CSFR, Granulocyte colony-stimulating factor receptor; HMGB1, High-mobility group box 1; HRP, Horse radish peroxidase; ICAM1, intercellular adhesion molecule 1; IHS, infant hepatitis syndrome; IL , Interleukin; LPS, lipopolysaccharide; MST, mean survival time; NK, natural killer; NLRP3, Recombinant NLR Family, Pyrin Domain Containing Protein 3; PMA, phorbol 12-myristate 13-acetate; RRV, rhesus rotavirus; SNP, single-nucleotide polymorphism; STAT3, signal transducer and activator of transcription 3; UMI, Unique molecular identifiers.

References

1 Hartley, J.L., Davenport, M. and Kelly, D.A. (2009) Biliary atresia. *Lancet* **374**, 1704–1713, https://doi.org/10.1016/S0140-6736(09)60946-6
2 Girard, M. and Panasyuk, G. (2019) Genetics in biliary atresia. *Curr. Opin. Gastroenterol.* **35**, 73–81, https://doi.org/10.1097/MOG.0000000000000509
3 Arikan, C., Berdeli, A., Kilic, M., Tumgor, G., Yagci, R.V. and Aydogdu, S. (2008) Polymorphisms of the ICAM-1 gene are associated with biliary atresia. *Dig. Dis. Sci.* **53**, 2000–2004, https://doi.org/10.1007/s10620-007-9914-1
4 Arikan, C., Berdeli, A., Ozgenc, F., Tumgor, G., Yagci, R.V. and Aydogdu, S. (2006) Positive association of macrophage migration inhibitory factor gene-173G/C polymorphism with biliary atresia. *J. Pediatr. Gastroenterol. Nutr.* **42**, 77–82, https://doi.org/10.1097/01.mpg.0000192247.55583.fa
5 Shih, H.H., Lin, T.M., Chuang, J.H., Eng, H.L., Juo, S.H., Huang, F.C. et al. (2005) Promoter polymorphism of the CD14 endotoxin receptor gene is associated with biliary atresia and idiopathic neonatal cholestasis. *Pediatrics* **116**, 437–441, https://doi.org/10.1542/peds.2004-1900
6 Zhao, R., Song, Z., Dong, R., Li, H., Shen, C. and Zheng, S. (2013) Polymorphism of ITGB2 gene 3′-UTR+145C/A is associated with biliary atresia. *Digestion* **88**, 65–71, https://doi.org/10.1159/000352025
7 Mezina, A. and Karpen, S.J. (2015) Genetic contributors and modifiers of biliary atresia. *Dig. Dis.* **33**, 408–414, https://doi.org/10.1159/000371694
8 Syal, G., Fausther, M. and Dranoff, J.A. (2012) Advances in cholangiocyte immunobiology. *Am. J. Physiol. Gastrointest. Liver Physiol.* **303**, G1077–G1086, https://doi.org/10.1152/ajpgi.00227.2012
9 Luo, Z., Jegga, A.G. and Bezerra, J.A. (2018) Gene-disease associations identify a connectome with shared molecular pathways in human cholangiopathies. *Hepatology* **67**, 676–689, https://doi.org/10.1002/hep.29504

10 Takeda, K., Noguchi, K., Shi, W., Tanaka, T., Matsumoto, M., Yoshida, N. et al. (1997) Targeted disruption of the mouse Stat3 gene leads to early embryonic lethality. *Proc. Natl. Acad. Sci. U.S.A.* **94**, 3801–3804, https://doi.org/10.1073/pnas.94.8.3801
11 Hillmer, E.J., Zhang, H., Li, H.S. and Watowich, S.S. (2016) STAT3 signaling in immunity. *Cytokine Growth Factor Rev.* **31**, 1–15, https://doi.org/10.1016/j.cytogfr.2016.05.001
12 Alonzi, T., Maritano, D., Gorgoni, B., Rizzuto, G., Libert, C. and Poli, V. (2001) Essential role of STAT3 in the control of the acute-phase response as revealed by inducible gene activation in the liver. *Mol. Cell. Biol.* **21**, 1621–1632, https://doi.org/10.1128/MCB.21.5.1621-1632.2001
13 Chakraborty, A. and Tweardyabc, D.J. (1998) Stat3 and G-CSF-induced myeloid differentiation. *Leuk. Lymphoma* **30**, 433–442, https://doi.org/10.3109/10428199809057555
14 Huang, Y.H., Chuang, J.H., Yang, Y.L., Huang, C.C., Wu, C.L. and Chen, C.L. (2009) Cholestasis downregulate hepcidin expression through inhibiting IL-6-induced phosphorylation of signal transducer and activator of transcription 3 signaling. *Lab. Invest.* **89**, 1128–1139, https://doi.org/10.1038/labinvest.2009.82
15 Nguyen-Jackson, H., Panopoulos, A.D., Zhang, H., Li, H.S. and Watowich, S.S. (2010) STAT3 controls the neutrophil migratory response to CXCR2 ligands by direct activation of G-CSF-induced CXCR2 expression and via modulation of CXCR2 signal transduction. *Blood* **115**, 3354–3363, https://doi.org/10.1182/blood-2009-08-240317
16 Panopoulos, A.D., Zhang, L., Snow, J.W., Jones, D.M., Smith, A.M., El Kasmi, K.C. et al. (2006) STAT3 governs distinct pathways in emergency granulopoiesis and mature neutrophils. *Blood* **108**, 3682–3690, https://doi.org/10.1182/blood-2006-02-003012
17 Zhang, R., Lin, Z., Fu, M., Guan, X., Yu, J., Zhong, W. et al. (2018) The role of neonatal Gr-1(+) myeloid cells in a murine model of rhesus-rotavirus-induced biliary atresia. *Am. J. Pathol.* **188**, 2617–2628, https://doi.org/10.1016/j.ajpath.2018.07.024
18 Zhou, Y., Zhou, B., Pache, L., Chang, M., Khodabakhshi, A.H., Tanaseichuk, O. et al. (2019) Metascape provides a biologist-oriented resource for the analysis of systems-level datasets. *Nat. Commun.* **10**, 1523, https://doi.org/10.1038/s41467-019-09234-6
19 Huang, W., Chen, Z., Zhang, L., Tian, D., Wang, D., Fan, D. et al. (2015) Interleukin-8 induces expression of FOXC1 to promote transactivation of CXCR1 and CCL2 in hepatocellular carcinoma cell lines and formation of metastases in mice. *Gastroenterology* **149**, 1053.e14–1067.e14, https://doi.org/10.1053/j.gastro.2015.05.058
20 He, Y.M., Li, X., Perego, M., Nefedova, Y., Kossenkov, A.V., Jensen, E.A. et al. (2018) Transitory presence of myeloid-derived suppressor cells in neonates is critical for control of inflammation. *Nat. Med.* **24**, 224–231, https://doi.org/10.1038/nm.4467
21 O'Hara, S.P., Splinter, P.L., Trussoni, C.E., Gajdos, G.B., Lineswala, P.N. and LaRusso, N.F. (2011) Cholangiocyte N-Ras protein mediates lipopolysaccharide-induced interleukin 6 secretion and proliferation. *J. Biol. Chem.* **286**, 30352–30360, https://doi.org/10.1074/jbc.M111.269464
22 Graf, D., Kohlmann, C., Haselow, K., Gehrmann, T., Bode, J.G. and Häussinger, D. (2006) Bile acids inhibit interleukin-6 signaling via gp130 receptor-dependent and-independent pathways in rat liver. *Hepatology* **44**, 1206–1217, https://doi.org/10.1002/hep.21368
23 Zhang, R.Z., Yu, J.K., Peng, J., Wang, F.H., Liu, H.Y., Lui, V.C. et al. (2016) Role of CD56-expressing immature biliary epithelial cells in biliary atresia. *World J. Gastroenterol.* **22**, 2545–2557, https://doi.org/10.3748/wjg.v22.i8.2545
24 Shivakumar, P., Sabla, G.E., Whitington, P., Chougnet, C.A. and Bezerra, J.A. (2009) Neonatal NK cells target the mouse duct epithelium via Nkg2d and drive tissue-specific injury in experimental biliary atresia. *J. Clin. Invest.* **119**, 2281–2290, https://doi.org/10.1172/JCI38879
25 Cacalano, N.A. (2016) Regulation of natural killer cell function by STAT3. *Front. Immunol.* **7**, 128, https://doi.org/10.3389/fimmu.2016.00128
26 Zhang, R., Lin, Z., Lui, V.C.H., Wong, K.K.Y., Tam, P.K.H., Lee, P. et al. (2017) Silver nanoparticle treatment ameliorates biliary atresia syndrome in rhesus rotavirus inoculated mice. *Nanomedicine* **13**, 1041–1050, https://doi.org/10.1016/j.nano.2016.11.013
27 Gotthardt, D., Putz, E.M., Straka, E., Kudweis, P., Biaggio, M., Poli, V. et al. (2014) Loss of STAT3 in murine NK cells enhances NK cell–dependent tumor surveillance. *Blood* **124**, 2370–2379, https://doi.org/10.1182/blood-2014-03-564450
28 Qiu, Y., Yang, J., Wang, W., Zhao, W., Peng, F., Xiang, Y. et al. (2014) HMGB1-promoted and TLR2/4-dependent NK cell maturation and activation take part in rotavirus-induced murine biliary atresia. *PLoS Pathog.* **10**, e1004011, https://doi.org/10.1371/journal.ppat.1004011
29 Zhao, T., Ren, H., Wang, X., Liu, P., Yan, F., Jiang, W. et al. (2015) Rituximab-induced HMGB1 release is associated with inhibition of STAT3 activity in human diffuse large B-cell lymphoma. *Oncotarget* **6**, 27816, https://doi.org/10.18632/oncotarget.4816
30 Xiao, Y., Liu, R., Li, X., Gurley, E.C., Hylemon, P.B., Lu, Y. et al. (2019) Long non-coding RNA H19 contributes to cholangiocyte proliferation and cholestatic liver fibrosis in biliary atresia. *Hepatology*, https://doi.org/10.1002/hep.30698
31 Hofmann, P., Sommer, J., Theodorou, K., Kirchhof, L., Fischer, A., Li, Y. et al. (2019) Long non-coding RNA H19 regulates endothelial cell aging via inhibition of STAT3 signalling. *Cardiovasc. Res.* **115**, 230–242, https://doi.org/10.1093/cvr/cvy206
32 Yang, L., Mizuochi, T., Shivakumar, P., Mourya, R., Luo, Z., Gutta, S. et al. (2018) Regulation of epithelial injury and bile duct obstruction by NLRP3, IL-1R1 in experimental biliary atresia. *J. Hepatol.* **69**, 1136–1144, https://doi.org/10.1016/j.jhep.2018.05.038
33 Mizushina, Y., Shirasuna, K., Usui, F., Karasawa, T., Kawashima, A., Kimura, H. et al. (2015) NLRP3 protein deficiency exacerbates hyperoxia-induced lethality through Stat3 protein signaling independent of interleukin-1beta. *J. Biol. Chem.* **290**, 5065–5077, https://doi.org/10.1074/jbc.M114.603217
34 Bai, H., Zhang, Q.F., Duan, J.J., Yu, D.J. and Liu, L.J. (2018) Downregulation of signal transduction and STAT3 expression exacerbates oxidative stress mediated by NLRP3 inflammasome. *Neural Regen. Res.* **13**, 2147–2155, https://doi.org/10.4103/1673-5374.241470
35 Park, J., Gores, G.J. and Patel, T. (1999) Lipopolysaccharide induces cholangiocyte proliferation via an interleukin-6-mediated activation of p44/p42 mitogen-activated protein kinase. *Hepatology* **29**, 1037–1043, https://doi.org/10.1002/hep.510290423
36 Chen, X.M., O'Hara, S.P. and LaRusso, N.F. (2008) The immunobiology of cholangiocytes. *Immunol. Cell Biol.* **86**, 497–505, https://doi.org/10.1038/icb.2008.37
37 de la Iglesia, N., Konopka, G., Lim, K.L., Nutt, C.L., Bromberg, J.F., Frank, D.A. et al. (2008) Deregulation of a STAT3-interleukin 8 signaling pathway promotes human glioblastoma cell proliferation and invasiveness. *J. Neurosci.* **28**, 5870–5878, https://doi.org/10.1523/JNEUROSCI.5385-07.2008
38 Grabner, B., Moll, H.P. and Casanova, E. (2016) Unexpected oncosuppressive role for STAT3 in KRAS-induced lung tumorigenesis. *Mol. Cell Oncol.* **3**, e1036199, https://doi.org/10.1080/23723556.2015.1036199

Clinical Science (2021) **135** 865–884
https://doi.org/10.1042/CS20201366

39 Bessho, K., Mourya, R., Shivakumar, P., Walters, S., Magee, J.C., Rao, M. et al. (2014) Gene expression signature for biliary atresia and a role for interleukin-8 in pathogenesis of experimental disease. *Hepatology* **60**, 211–223, https://doi.org/10.1002/hep.27045

40 Gao, Y., Basile, J.I., Classon, C., Gavier-Widen, D., Yoshimura, A., Carow, B. et al. (2018) STAT3 expression by myeloid cells is detrimental for the T-cell-mediated control of infection with Mycobacterium tuberculosis. *PLoS Pathog.* **14**, e1006809, https://doi.org/10.1371/journal.ppat.1006809